Del Moral, A., M.C. Llasat, T. Rigo, Atmospheric Research, 238 (2020) 104863
DOI: 10.1016/j.atmosres.2020.104863

Connecting flash flood events with radar-derived convective storm characteristics on the Northwestern Mediterranean coast: knowing the present for better future scenarios adaptation

Anna del Moral[a,c], María del Carmen Llasat[a,c], Tomeu Rigo[b]

[a] *Department of Applied Physics, University of Barcelona, Barcelona, Spain*
[b] *Meteorological Service of Catalonia, Barcelona, Spain*
[c] *Water Research Institute of the University of Barcelona, Spain*

Abstract

The northwestern Mediterranean coast is one of the areas most affected by flash floods and adverse weather, where also global climate scenarios are predicting an increase of precipitation extremes. This, along with the sea-level rise and the associated potential infrastructure and economical loses, represent a major risk for coastal settlements, as the one studied in this work: a major touristic area in the southern coast of Catalonia. The objective of the present paper is, thus, to understand in-depth the behavior of convective activity in the area and its link with flash flood events, to improve adverse and severe weather early warning systems in a rapidly changing weather as an adaptation measure. With this purpose, the study focuses on the period 2014-2018, analyzing the convective cells and storm motion in the region of study, through the new identification and tracking algorithm developed by the authors and applied in the Meteorological Service of Catalonia. The results show that the area is mostly affected by shallow but efficient convection, probably embedded in major weather systems with high precipitation rain rates, which tends to saturate the catchments and produce flooding. The work also shows the role of the topography as a triggering factor for storms outside the convective season, as a key feature for the convergence lines organization, and as a capping for stationary cells upstream. Improvements on the current warning system, such as different precipitation thresholds considering the time of exposure to that rain, as well as a further study are also presented as main results. These results can be extrapolated and applied to other regions affected by the same kind of heavy precipitation and flash floods.

Keywords: Flash floods, coastal floods, nowcasting, storm tracking, convective precipitation, meteorological radar, Salou, Mediterranean coast

1.Introduction

The Mediterranean climate is typically characterized by sunny days and warm temperatures during the majority of the year due to the influence of the sea, attracting a significant amount of tourism

from around the world. During late summer and autumn, this coincides with the most frequent and intense convective activity in the western region of the Mediterranean Sea (Llasat et al., 2010b; Rozalis et al., 2010; Ducrocq et al., 2014), posing risks during the peak of the touristic season. One of the most affected regions is Catalonia (north east of the Iberian Peninsula, Fig.1), where convective activity bearing severe weather and intense rainfall is favored due to the combination of the complex topography and the proximity to the sea (see, for instance, Barnolas and Llasat, 2007; Rigo and Llasat, 2016; Cortès et al., 2017; Farnell et al., 2017; and Rodríguez and Bech, 2018). Specifically, the east coast of Spain, where the population increases by 10% during summer from tourism alone (Llasat et al., 2010a), is largely affected by this increased strong convective activity. This populous and dense region is thus positioned in a hot spot prone to suffer from floods and other catastrophic events, along with other Mediterranean coastal areas such as the southeast of France, the northwest of Italy or the Croatian coast. For instance, the EM-DAT international disaster database (http://www.emdat.be/) lists 85 billion Euros in damages related to river floods and flash floods since 1900 in the countries surrounding the Mediterranean Sea (Gaume et al., 2016). Also, Petrucci et al. (2019) identify 812 fatal floods with 2466 fatalities for the period 1980–2018 in eight Mediterranean countries plus the Czech Republic, of which most of them occurred outdoor.
Several studies have revealed that future global climate scenarios predict an increase of precipitation extremes in different regions of the world during the coming decades (Seneviratne et al., 2012). More concretely, Toreti et al. (2013) and Toreti and Naveau (2015) found that heavy rainfall events in the Mediterranean basin are likely to intensify by up to 20% which, along with other resultant issues such as sea-level rise, the robust climate change signal of a faster temperature increase compared to the world average and the associated potential infrastructure and economical loses, represent a major risk for coastal settlements (Cramer et al., 2018, Tramblay and Somot, 2018). In this sense, the improvement of early-warning systems is a key element from the hydro-meteorological perspective, especially in highly populated and urban areas. This, along with a better risk awareness, could avoid the high number of casualties.

Cortès-Simó et al. (2018) demonstrate that 30-minute rainfall is highly correlated with flash flood events in such areas. This agrees with Togersen et al. (2015) and Spekkers et al. (2013), who show that there is almost a direct relation between intense, short rainfall events and insurance data reflecting claims that affect private property. There is thus a need to prioritize current efforts of the meteorological community to understand in depth the behavior of convective cells associated with intense rainfall events in these Mediterranean coastal areas.

Nowcasting of convective cells producing heavy rainfall and severe weather depends on fast and reliable identification and diagnosis tools to provide clear and important information to aid operative forecasters in their decision-making process. Products derived from meteorological radars have thus become a common instrument integral to convective research and the operative community. In particular, radar-based nowcasting (i.e. Dixon and Wiener, 1993; Han et al., 2009; del Moral et al., 2018a) is a diagnostic and analysis tool able to run in real-time and provides a significant amount of information about precipitating structures, identifying convective cores, tracking their life cycle, and forecasting their future paths at a high temporal and spatial resolution. Several studies have demonstrated the benefits of the combination of radar nowcasting and auxiliary tools such as lightning or vertical atmosphere profiles, among other (i.e. Steinaker et a., 2000; Hu et al., 2019; Shi et al., 2019). These integrated systems enhance the ability to analyze

and greatly improve the forecast skill of severe or adverse weather phenomena early warning systems. However, there still exists a lack of a complete understanding of the local and internal dynamics of these thunderstorms. The research community has worked towards identifying the features controlling storm severity while also investigating interactions between cells and how cells interact with their surrounding environment (e.g. topography, mesoscale boundaries, sea-land interaction), which may influence the evolution, duration, direction, or area affected (del Moral et al., 2018b). Furthermore, in a quickly changing climate encompassing global warming scenarios with increased adverse weather events in coastal areas, it is necessary to perform quasi-individual studies in local regions with potential high-risk factors since interactions between social, economic, hydrological and meteorological fields are starting to play a major role. In this sense, for instance, the results obtained in this paper could be applied to other regions with similar features of heavy rainfalls that produce flash floods as it has been commented before. This is the case, for example, of Liguria (Italy), where convective activity plays a major role (see, Fiori et al., 2014; Braud et al., 2014; Gaume et al., 2016).

The work presented here aims to start investigating some of these outstanding questions in a region of the Catalan coast that has been identified as a potential risk area associated with an elevated number of flash flood events and high vulnerability (Cortès et al., 2018). For instance, what are the characteristics of the convective cells affecting the region (e.g. vertical development, duration and motion)? Are cells related to deep or shallow and more efficient convection? Do cells remain relatively shallow with efficient microphysical precipitation processes, or do they instead grow into deep convective towers? What is the role of the sea and the topography in cell initiation and motion? Are flash floods strictly related to high rainfall rates? As part of the Spanish project M-CostAdapt (CTM2017-83655-C2-2-R), and therefore a part of the Mediterranean community, our main goal is to utilize a radar-based perspective to better understand the region's convective activity. The work additionally acts as a starting point for future and broader meteorological studies in other potential areas susceptible to adverse and severe weather events. The document is divided as follows: first, we present the area of study and the datasets utilized. The third section discusses the methodology, from the filtering of case studies to the application of the nowcasting algorithm which has been the main diagnosis tool used in this project. The fourth section includes results and discussion, which are divided into the following three analysis subsections: convective cells, the time dependent features (life cycle characteristics) and the three important flash flood events that have impacted the area. Finally, the fifth section presents our conclusions.

2. Study area and data

2.1 Characteristics of the regions of interest

Fig. 1 shows the regions of study, hereafter denoted Regions of Interest (ROIs). The analysis is focused on the southern coast of Catalonia (NE of the Iberian Peninsula, Fig. 1a) referred to as ROI1, and a more focused, smaller region centered over the Salou municipality (ROI2) for more detailed analysis (Fig. 1b). ROI1 is typically affected by surface freshwater floods and flash floods (Llasat et al., 2014), which is a consequence of high frequency, local, and temporally short convective events producing heavy rainfall (Llasat et al., 2007) as well as height variations of the local mountain ranges (from 0 to 600 m in less than 10 km or from 0 to 1,200 m in less than 30 km) acting as a triggering mechanism for convection (Fig. 2a). The steep orography also influences

in the hydrologic part, because of the short-time response of the basins. Specifically, 29 flood events have occurred between 1981 and 2015 in Salou, impacting the town itself and several camping and vacation resorts surrounding the region that are crossed by streams flowing into the Mediterranean Sea (Fig. 2b). Although autumn floods are usually associated to synoptic situations characterized by cyclonic structures and southeast advections, local flash floods that occurred primarily in summer and early autumn are not reflected at synoptic scale, being mainly associated to mesoscale factors (Gilabert and Llasat, 2017).

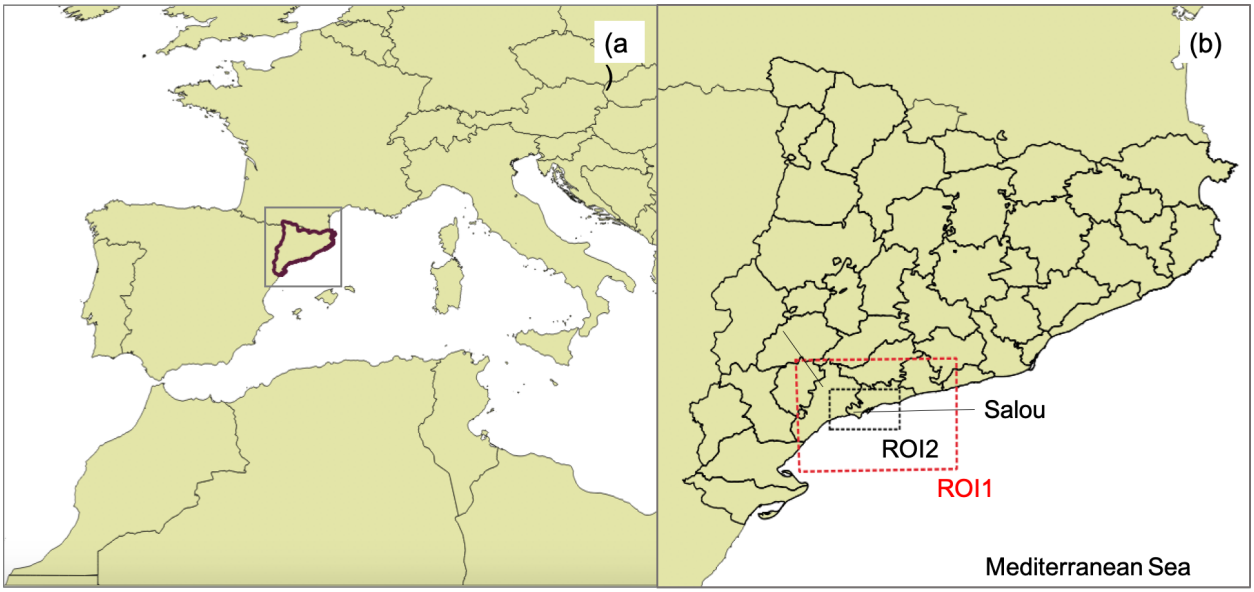

Figure 1: Regions of Interest (ROIs); (a) Catalonia (NE of the Iberian Peninsula) and (b) zoomed view of the two regions studied (ROI1 and ROI2).

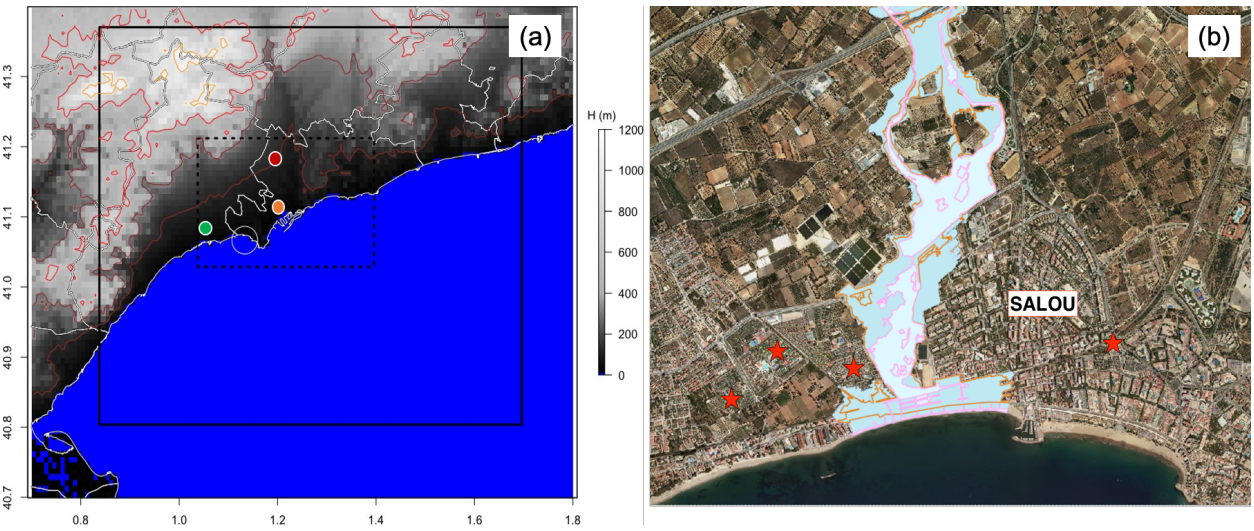

Figure 2: (a) Topography of ROI1 (solid black line rectangle) and ROI2 (dotted black line rectangle) presented in Fig. 1b. The town of Salou is marked with a white circle. The light brown,

brown, red and orange lines indicate the 100, 300, 600 and 1000 m contours, respectively. The color circles represent the three Automatic Weather Stations (AWS) of the Meteorological Service of Catalonia (SMC); U6 in green, XE in orange and VQ in Red. (b) Flood hazard map of the Salou stream "Torrent de Barenys" for different return periods; T=10 years (pink contour), and T=100 years (orange contour), T= 500 years (blue area). Red stars represent camping and vacation resorts (source: ACA, 2019).

Interest in Salou is motivated by its status as one of the most important touristic towns in Catalonia because of its beaches. Although the municipality only has 26,775 inhabitants (2018) in an area of 15.13 km^2 (density of population of 1,769.7 inhab./km^2), overnight visits approach nearly 8 million annually (i.e. 7,994,205 in 2017). Shown in Fig. 2b, the major urbanistic and touristic settlements are surrounding the stream "Torrent de Barenys" and thus lie within a potential high-risk flood area. The different return periods shown in Fig. 2b (10, 100 and 500 years) correspond to a precipitation amount of 110.4 mm, 187.4 mm and 249.1 mm and a discharge (volumetric flow rate from streams to the sea) of 57.3 $m^3 \cdot s^{-1}$, 178.1 $m^3 \cdot s^{-1}$ and 307 $m^3 \cdot s^{-1}$, respectively. It is observed that an important part of Salou is constructed over a flood prone area which considers not only flooding as a result of "in-situ" rain but also upstream rain, affecting the headwaters of the "Torrent de Barenys". The cases presented in the final part of this paper show these different possibilities, highlighting the flood of the stream when it barely rains over Salou. This is one of the most dangerous situations, since the population is off guard and with a low temporary response.
More revealing information is found through a lightning analysis, which, according to the database from 2000-2018 of the Spanish Agency of Meteorology (AEMET, *Agencia Española de Meteorología*), shows that the coast of ROI1 (Salou and surroundings) is the most affected by lightning compared to the rest of the Catalan coast (Fig. 3). This supports the understanding that frequent events affecting the area are also of vigorous convective behavior, which implies additional risks to the area, such as possible severe weather (e.g. strong winds, hail, and even tornadoes). Frequent cloud-to-ground lightning also impacts electrical networks and increases the potential for forest fires, but also poses a serious risk to human safety. The coupling of these convective meteorological phenomena and the increasing population and vacation resort settlements during the summer and autumn seasons makes this area extremely vulnerable to adverse and severe weather, and thus motivates the study of these events along the western Mediterranean coast. The unfortunate consequence is Salou's positioning being a paradigmatic example of a touristic Mediterranean village placed in a flood-prone area, and as such deserves special attention for future climate-related adaptation.

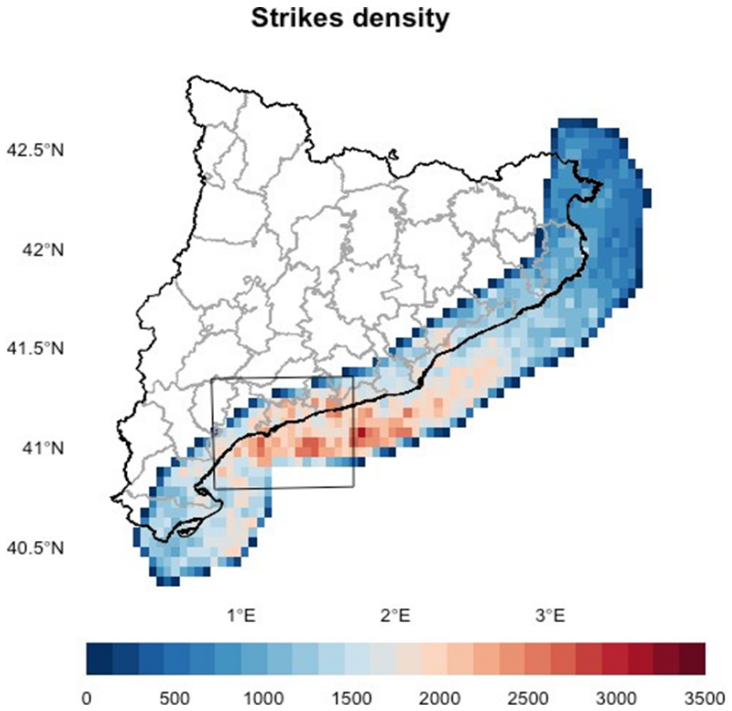

Figure 3: Cloud-to-ground (CG) strike density over the Catalan coast from the period 2000-2018. The main region of study (ROI1) is marked with a black rectangle. The map has been constructed with the AEMET CG lightning database data (the only one that the agency provides).

2. 2 Data used

The study presented here is based on radar data or its derived products, which are described in the following subsections.

2.2.1 Daily and hourly accumulated precipitation fields

Daily and hourly rainfall fields for the entire period of study (2014-2018) have been used as a preliminary filter for case study selection. These 24-h and 1-h Quantitative Precipitation Estimation (QPE) fields are calculated by combining the accumulated rainfall field obtained via the corrected reflectivity data from the Hydrometeorological Integrated Forecasted Tool (EHIMI, Corral et al., 2009) with the rainfall data from the Automatic Weather Stations (AWS) Network (hereafter XEMA, *Xarxa d'Estacions Meteorol`ogiques Automàtiques*) of the Meteorological Service of Catalonia (*Servei Meteorològic de Catalunya*, SMC) which is made up of 180 AWS. The combination is made by means of a co-kriging interpolation (Trapero et al., 2009; Velasco-Forero et al., 2009), and the corrected reflectivity is obtained from the Meteorological Radar Network of the SMC (hereafter XRAD, Xarxa de Radars Meteorològics),explained in Section 2.2.2.

2.2.2 Radar reflectivity fields

Composite reflectivity fields from the XRAD (Altube et al., 2015) during the period 2014-2018 has been used. XRAD incorporates four C-band (5.600-5.650 MHz or 53.57-53.10 m) Doppler

radars with single polarization. The data used in the present study is the volumetric composite product of 10 Constant Altitude Plan Position Indicators (CAPPIs), which are made of horizontal cuts of interpolated data at a fixed altitude, going from 1 km to 10 km AGL, in 1 km by 1 km, with a spatial and temporal resolution of 2x2 km^2 and 6 minutes, respectively (Rigo et al., 2010).

3. Methodology

The core of this study is performed by analyzing results after applying an object-oriented convective cell identification and tracking algorithm to the 6-minute composite volumetric reflectivity data set for the period 2014-2018. However, to optimize computational time, a preliminary filter based on the daily and hourly accumulated rainfall fields has been applied to reduce the initially more than 438,000 volumetric fields (explained in detail in Section 3.1).

3.1. Daily and hourly preliminary filter

This procedure consists in the application of the daily filter shown in del Moral et al. (2017), in order of identifying "potentially convective" days over a total of 1,826 daily maps covering ROI1 for the entire period. We identify a potentially convective day having, at least, one structure with a maximum accumulated precipitation of over 15 mm/24 hours, where a structure is defined by a precipitating area of, at least, 6 km^2. This reduces the daily starting dataset to 250 files, and consequently 6,000 hourly files. Then, the hourly filter is used within the same area (ROI1), with a threshold for identifying the precipitation structures of 1mm/1hour and with no area restriction. This lessen the dataset to 1,290 final files. In terms of 6-minute volumetric fields, it results in 12,900 10-level CAPPI volumes for processing with the identification and tracking algorithm.

3.2. Identification and tracking of convective cells

The identification and tracking of the convective cells is performed by applying the algorithm described in del Moral et al. (2018a), which is an improved version of the current operative algorithm at the SMC (Rigo and Llasat, 2016) and is based on the Storm Cell Identification and Tracking algorithm (SCIT, Johnson et al., 1998). This new object-oriented 3D identification and centroid-tracking algorithm is a 4-step version updated for severe weather surveillance purposes to identify severe storms that present anomalous motion (split and/or merge) that tend to affect the Catalan area during the convective season. The algorithm contains four main stages: pre-processing, planar identification (2D), volumetric (3D) identification and tracking. Primary features of this algorithm are summarized in Table 1 (see del Moral et al., 2018a for a detailed explanation).

Module	Feature	Action	Result
Pre-processing	Mask to remove echoes ≥ 75 dBZ, especially around the radar location	Added new	-Remove false echoes from anomalous propagation and interferences

2D identification	Queen's case Pixel labelling technique (8 directions)	Changed from Rook's case (4 directions)	-Less restrictive object construction
2D identification	Two seven-threshold (30,35,40,45,50,55,60 dBZ) filter. Applied top-down and bottom-up in every CAPPI level	Added the second threshold	-Retrieve structures that are more realistic in shape and size -Identify different cores in the same structure.
3D identification	Overlapping of 2D objects	Changed from centroid connection	-Identifies, in advance, possible splitting/merging processes
Tracking	Dynamic distance thresholds based on area and continuity of cells features	Changed from centroid distance matching	-More realistic and continuous tracks -Continuity of cell track during life cycle -Splitting/merging warnings

Table 1: Main identification and tracking features improved from the SMC algorithm version.

After identifying the convective cell, these are tracked throughout the entire life cycle to obtain time- and direction-dependent features. These meteorological structures are called henceforward "storms", which are defined as the connection of different convective cells through radar frames (and thus through time). We thus describe direction- and time-dependent features over ROI1 by accounting for the velocity in $m \cdot s^{-1}$ and the duration in minutes. Importantly, this framework allows the identification of convective initiation (CI). Finally, we compare the convective features of the ROIs with features identified in notable flash-flood events that have impacted Salou, which allows us to establish key characteristics of these flood-producing storms.

4. Results and discussion

This section contains three subsections: (1) the analysis of the convective cells, which includes a study of the outlier values of some features, (2) the entire storm life cycle climatology, and (3) the comparison with important flash-flood events in the area. Section 4.1 includes a study of the outlier values of some features, in order to determine if they correspond to real cells or not. Although those values might not skew a lot the distribution, it is necessary to know if those outlier values correspond to real storms that might pose much higher safety risk.

4.1 Convective cells

- Seasonal distribution

The spatial distribution of convective cells, by season, within ROI1 for the period 2014-2018 is shown in Fig. 4, where the distribution is the number of cell centroids inside a pixel of a 4 km^2

area. The number of convective cells varies strongly depending on the season of the year. Autumn (October to December) presents the highest number of cells (Fig. 4d), with areas affected by more than a total of 4,000 cells, which coincides with the convective season in the coastal area of Catalonia (Aran et al., 2015). Spring and summer (April to June and July to September, respectively) record maximum values above 1,000 cells (Fig. 4b and c). Note that the color bars in each subpanel of Fig. 4 are scaled according to the maximum value and thus differ from one subpanel to another. Winter (January to March) is the season with smallest amount of convective activity, with a maximum value of only 150 cells during the studied period and large areas without a single cell.

Having in mind the topography presented as contour lines, Fig. 4 shows clear differences in the pattern distribution regarding the first and second half of the year. During spring (Fig. 4b), the convective activity is mostly concentrated inland, mainly over the mountainous area (top left corner of Fig. 4b). This indicates that the sea surface is colder compared to land temperature. In this context, the orography plays a key factor in the convective process, likely as a triggering mechanism or an aid in creating convergence lines for organizing thunderstorms. Contrarily, both summer and autumn (Fig. 4c and d, respectively) show a greater concentration over the sea. This is due to the high surface temperature of the Mediterranean Sea, which feeds the lower atmosphere with a large amount of moisture and enables the cells to grow and develop more rapidly (Pastor et al., 2015).

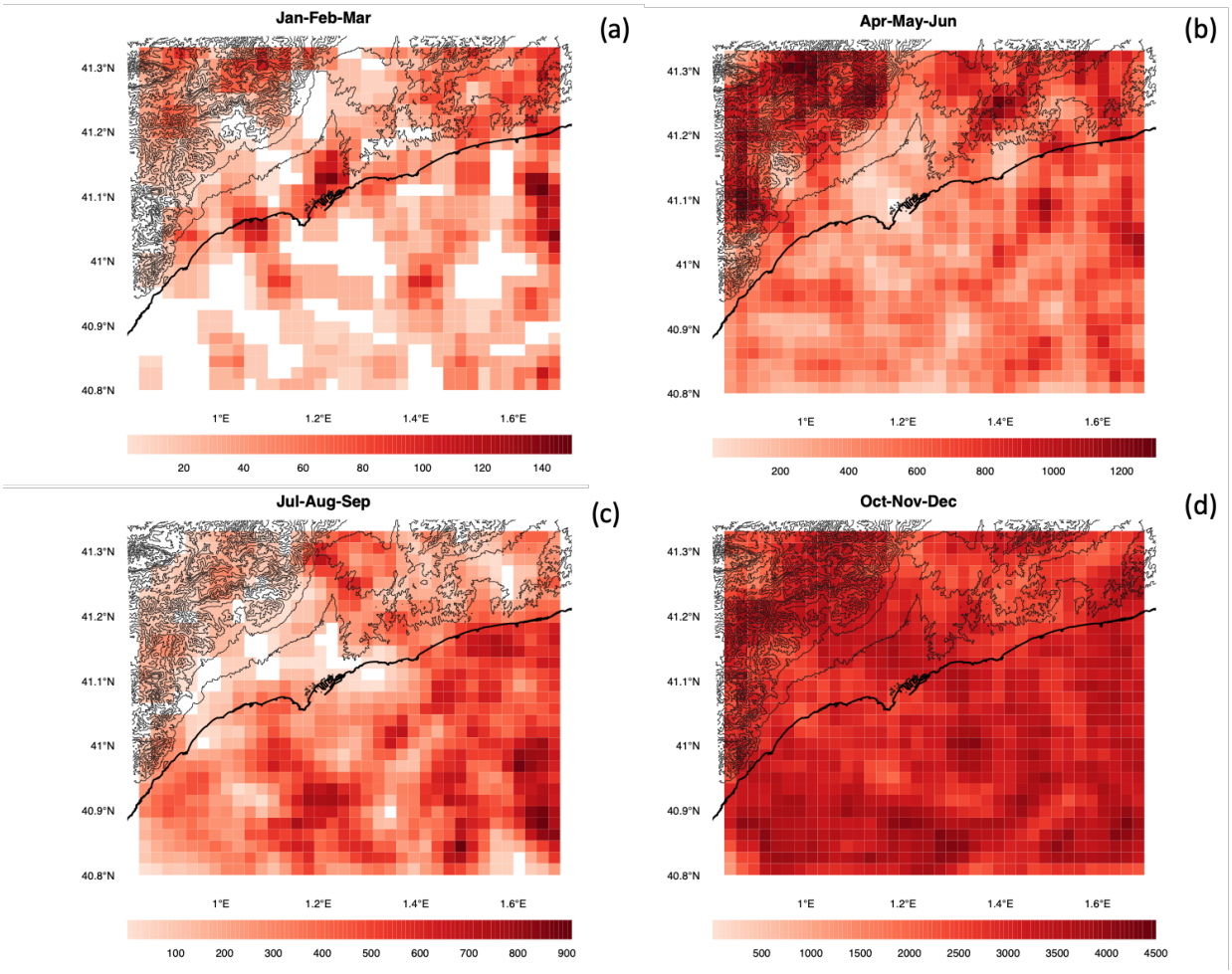

Figure 4: Spatial and seasonal distribution (number of cells in a 4x4 pixel) of convective cells between the period 2014-2018 in ROI2; (a) winter (January through March); (b) spring (April through June); (c) summer (July through September) and (d) autumn (October through December). Pixel maps have been smoothed by applying a 3x3 Gaussian filter around every pixel. Each pixel corresponds to an area of 4 km^2, and the contour lines indicate the topography (every 100 m).

-Convective cells characteristics

The main features of the cells, including maximum reflectivity (ZMAX), convective cell top height (HTOP, in km) and the highest height of the 40 dBZ echo (HTOP40, in km), are shown in Fig. 5. First, it can be seen the high variation of cells identification along the year: September and October are the only months on which it has been identified convective cells for all the years. Also, these months present the highest variation in all the characteristics, which demonstrates that the convective season takes place during those months. The median value for the core height is 3 km for all years (Fig. 5a), except for 2014 during which it is even lower (2 km). In addition, the interquartile range is 2-4 km for all years, indicating that the top of the cell is typically located at low levels. This is representative of shallow convection, frequent in the Catalan coast where usually thunderstorms' cell tops don't exceed 6 km (Ballart, et al., 2009). This is the opposite to most of the thunderstorms producing severe weather phenomena in other regions of Catalonia,

such in the plains, where these present higher tops, even exceeding 10 km (see, for instance, del Moral et al., 2017, Rigo et al., 2010, or Rigo and Llasat, 2004). The median ZMAX for all years is between 40 and 45 dBZ, which represent values likely resulting from high precipitation efficiency (rimed ice particles like hail or graupel generally produce higher reflectivity values of up to 60 dBZ). It is also found that the echo tops of 30 dBZ do not exceed 8 km of altitude (most of the cases under 5 km) and that high reflectivity values (over 40 dBZ) are located at low levels. According to Doswell et al. (1996), the high precipitation concept is referred to a high relationship between the output and input water fluxes in a thunderstorm. Therefore, values over 40 dBZ indicate that most of the input water flux is converted into rainfall which, from a spotter point of view, would result really intense and with large drop size. The yearly distribution of ZMAX shows that during 2017, cells generally produced lower values of reflectivity. The highest ZMAX values occurred during 2018, which was also the year in which Catalonia, and especially the Salou area, recorded extreme precipitation values and several floods during autumn season. Also, that year was the most convective one in average, since a high amount of cells, with slightly higher values of ZMAX, HTOP and HTOP40 occurred (Fig.5). Table 2 shows the remarkably high maximum values of 24-hr precipitation for 2018. The three AWS within ROI2 recorded more than 100 mm in 24 hours in October, with two records occurring during the same event—the storm on October 14, 2018.

Year	Station	Annual Mean [mm]	Annual Max/24h [mm]	Date of Max/24h [DD/MM]
2014	VQ	638.5	62.9	16/09
	U6	418.9	30.5	30/11
	XE	544.8	46.5	30/03
2015	VQ	549.5	95.9	02/09
	U6	382.8	45.9	02/09
	XE	471.5	43.6	29/09
2016	VQ	500.3	57.6	27/11
	U6	481.8	97.7	16/12
	XE	425.1	59.4	27/11
2017	VQ	339.9	45.4	24/03
	U6	273.1	50.6	18/10
	XE	276.9	39.3	24/03
2018	VQ	848.4	100.2	14/10
	U6	682.5	112.6	09/10
	XE	762.8	101.2	14/10

Table 2: Maximum values of precipitation in 24h [mm] and mean annual precipitation [mm] for the period of study (2014-2018) for the three Automatic Weather Stations from the XEMA network of the SMC within ROI2.

The 40 dBZ echo tops (Fig. 5c) are generally located at almost the same height as the cell tops (Fig. 5a), with the interquartile range generally between 2 and 3 km. Both results demonstrate that the region is usually affected by convective cells with low vertical development (shallow convection) and a high precipitation efficiency, where the intense cores occupy low- and mid-levels of the troposphere.

According to the single cell conceptual model (Chisholm and Renick, 1972; Wilk et al., 1977), this behavior agrees with cells in later mature stages. During that period (late mature) the updraft

starts to dissipate, and the core is displaced to low levels. This stage starts where a dominant downdraft forms and the precipitation reaches the surface shortly after. It is important to note that this conceptual model is also used to describe other types of convective organization such as multicell or supercells (Doswell, 2001; Kumjian and Ryzhkov, 2008).

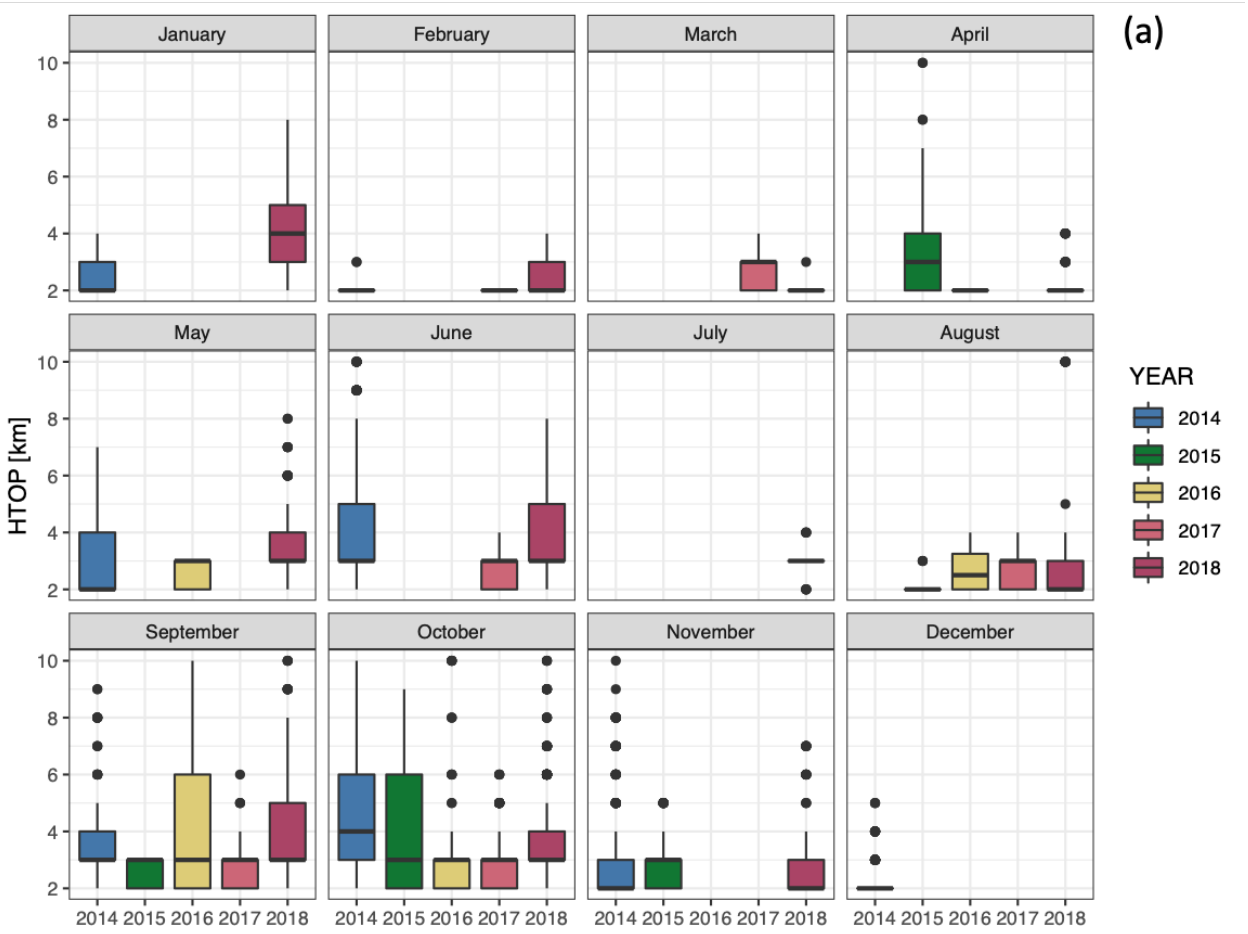

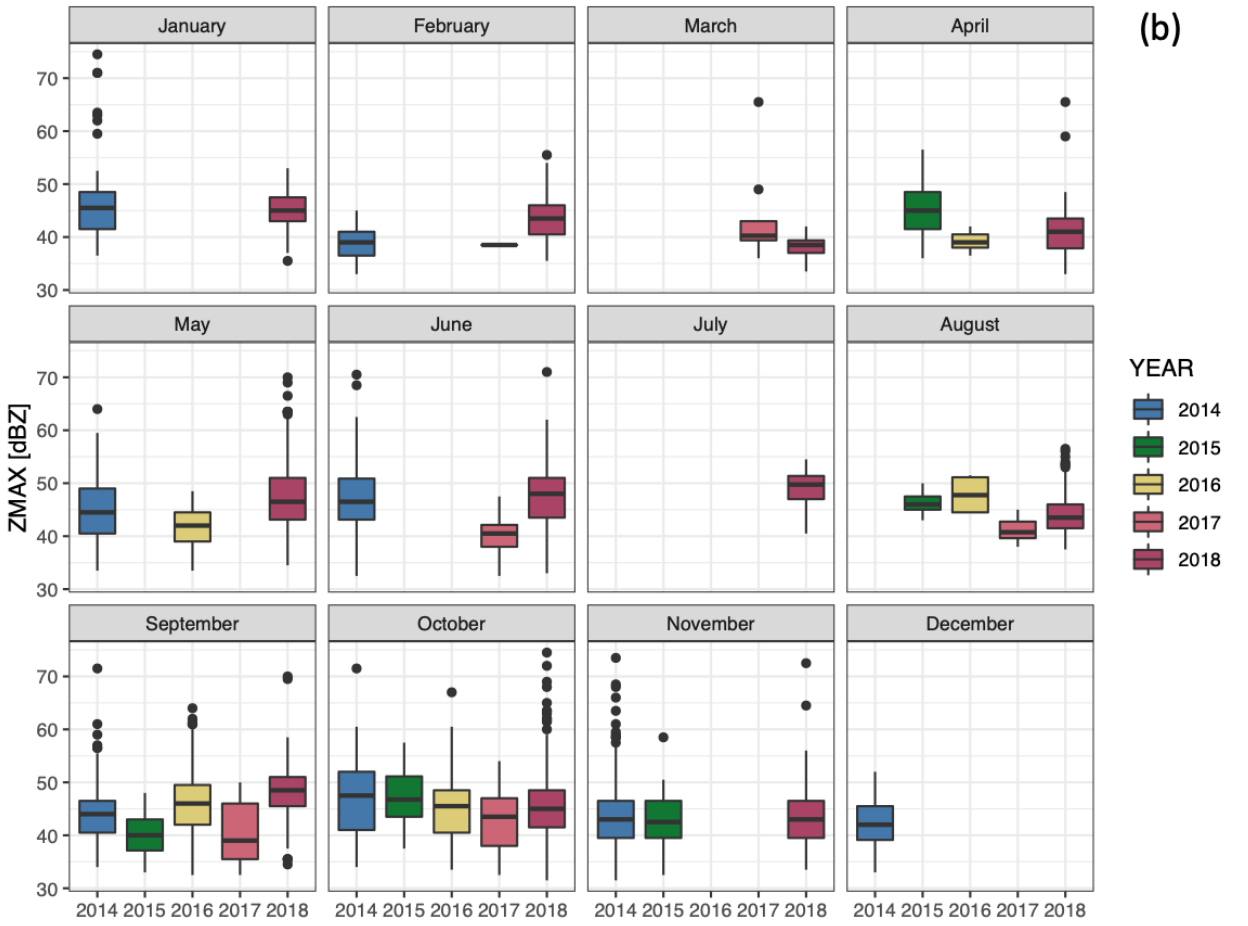
(b)
January
February
March
April
May
June
July
August
September
October
November
December
ZMAX [dBZ]
70
60
50
40
30
2014 2015 2016 2017 2018
YEAR
2014
2015
2016
2017
2018

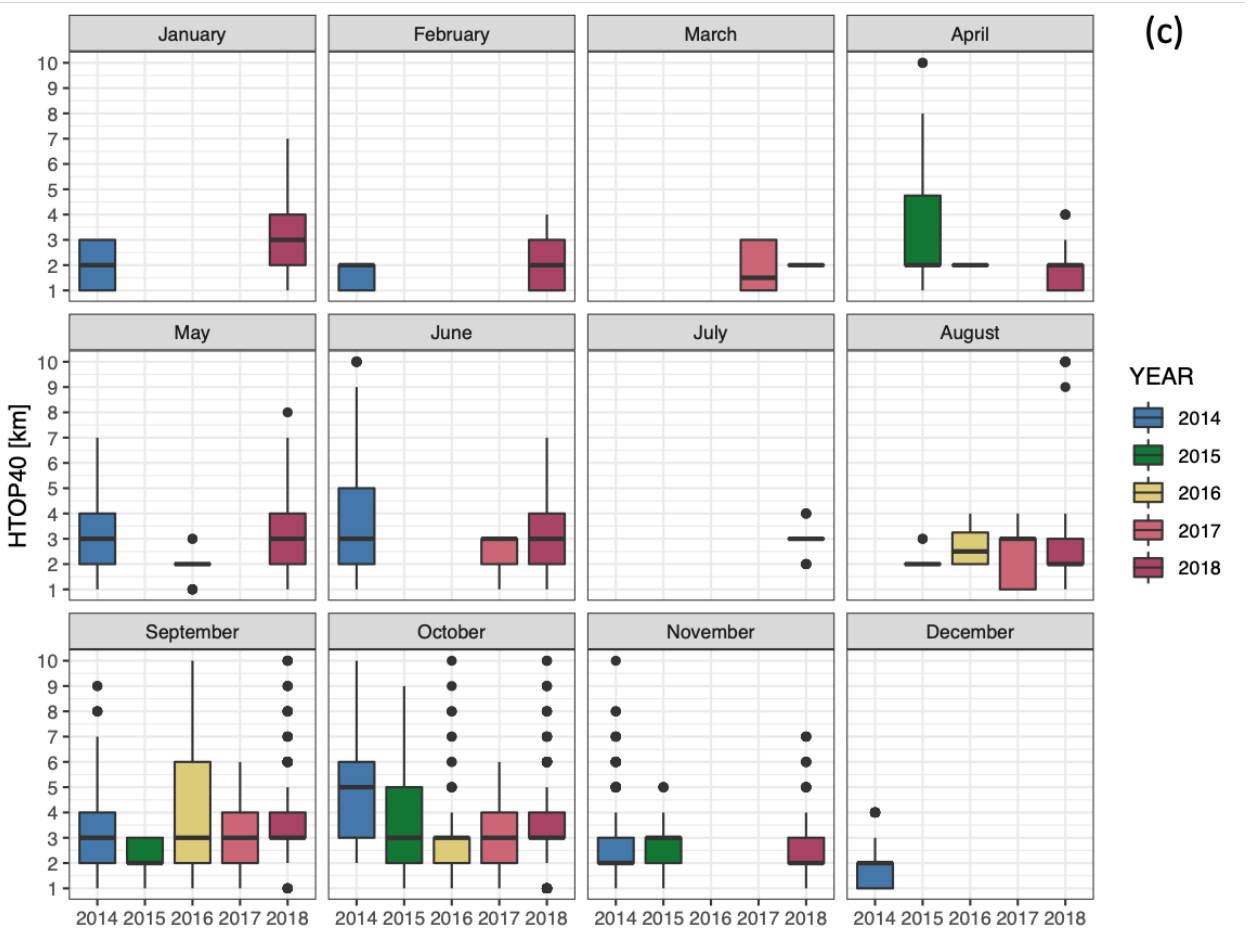

Figure 5: Boxplots of convective cells characteristics separated by year and month; (a) convective cell top height, HTOP [km]; (b) maximum reflectivity, ZMAX [dBZ] and (c) maximum height of 40 dBZ echoes, HTOP40 [km].

- *Outliers analysis: extreme values*

The distributions in Fig. 5 show that some outlier cells have a ZMAX greater than 59 dBZ and an HTOP greater than 8 km. Using these values as a threshold for identification, a total of 19 outlier cells were found that formed on 6 different days, as shown in Fig. 6. These outliers coincide with large convective cells, mostly concentrated along the coast or offshore, that have extremely high reflectivity values and deep vertical development (Fig. 5). These features suggest the occurrence of deep convection in some concrete events, in which the updrafts tend to reach above the freezing level where the coexistence of liquid and ice phase particles results in higher reflectivity.

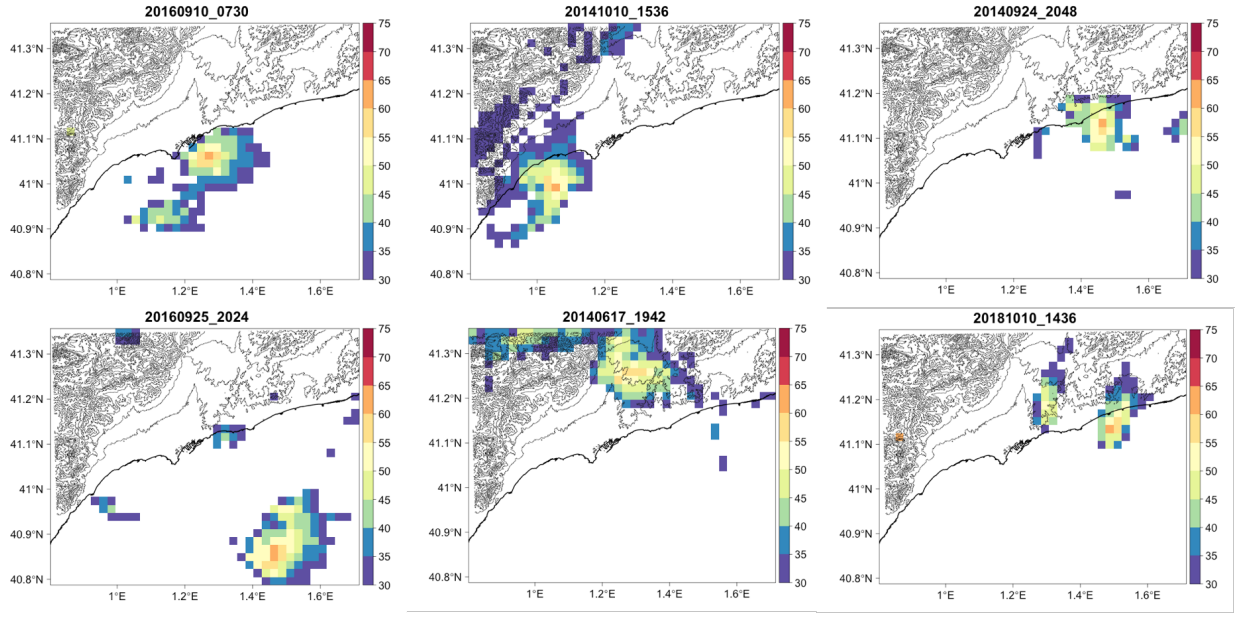

Figure 6: Maximum reflectivity (ZMAX) for the six different convective cells with outlier values (high ZMAX, HTOP and HTOP40). Color bar represents reflectivity in dBZ.

Another outlier pattern was found when analyzing the reflectivity values in Fig. 5; these include 19 cells with very high reflectivity values but also relatively low echo top heights of 2 km, which are part of 11 different days. A representative sample of those outlier cells is shown in Fig. 7. These outlier values with ZMAX above 59 dBZ, most reaching values greater than 60 dBZ, do not represent real meteorological pixels, and therefore are not part of a cell core. The reflectivity gradient is much stronger than the case of the outliers in Fig. 6; those extremely high values of reflectivity are surrounded by neighbor values which in all the cases differ by, at the very least, 20 dBZ. Furthermore, it is important to note that the position of the maximum values is located over the same area (framed in black in Fig. 7). Comparing Fig. 7 with Fig. 2a, this area is shown to be within the mountainous region. This suggests possible anomalous propagation of radar echoes or electromagnetic interferences with, for instance, electric towers or wind farms. For that reason, these outlier values have been considered to be unreal convective cells, and therefore are discarded as a real representation of the convective activity in the area.

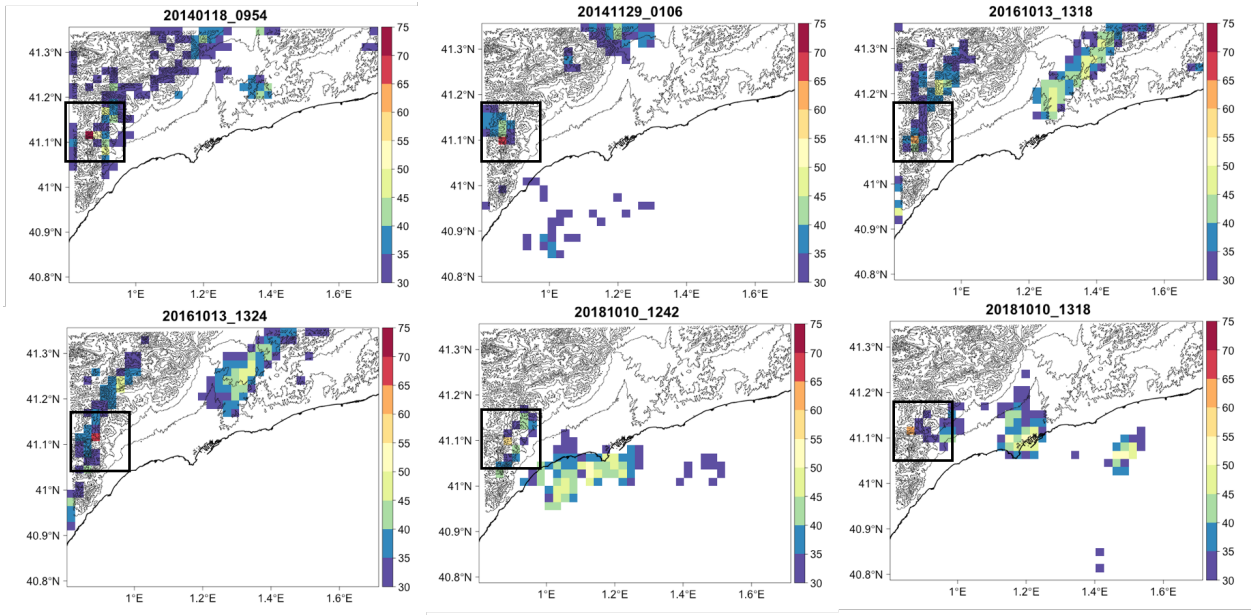

Figure 7: Maximum reflectivity of 6 radar frames with the second group of outliers (high ZMAX and low HTOP and HTOP40 values). Pixels with the highest reflectivity value are framed with a black box. Color bar represents reflectivity [dBZ].

4.2 Storm life cycle

4.2.1 Storm initiation

Understanding the nature of the storms that affect ROI1 requires determining the location of initiation. Fig. 8 thus shows the spatial distribution, separated by season, of the storm initiation (henceforward, SI) expressed in number of cells in a pixel of 4 km^2. This is the location of the first identified 3D cell that encompasses the entire storm after tracking. The spatial distribution, as well as the SI density, follow a similar pattern that the total number of cells by pixel shown in Fig. 4, although in the SI case the region analyzed is extended to surrounding areas (ROI1 instead of ROI2, in order to identify the role of topography in the initiation). Note that the maximum SI concentration is located inland during winter and especially during spring (Fig. 8a and b, respectively), which would coincide with the triggering effect from orography. On the other hand, for the warm seasons when the sea surface temperature is high, SI moves offshore, where convergence lines can be seen in the area (Fig. 8c, d and e). This would coincide with the usual patterns (Pineda et al., 2007, Rigo et al., 2010) during the convective season in the Catalan area, where several easterly flows affect the coast and when several convergence lines can be formed perpendicular to the coast (east to west).

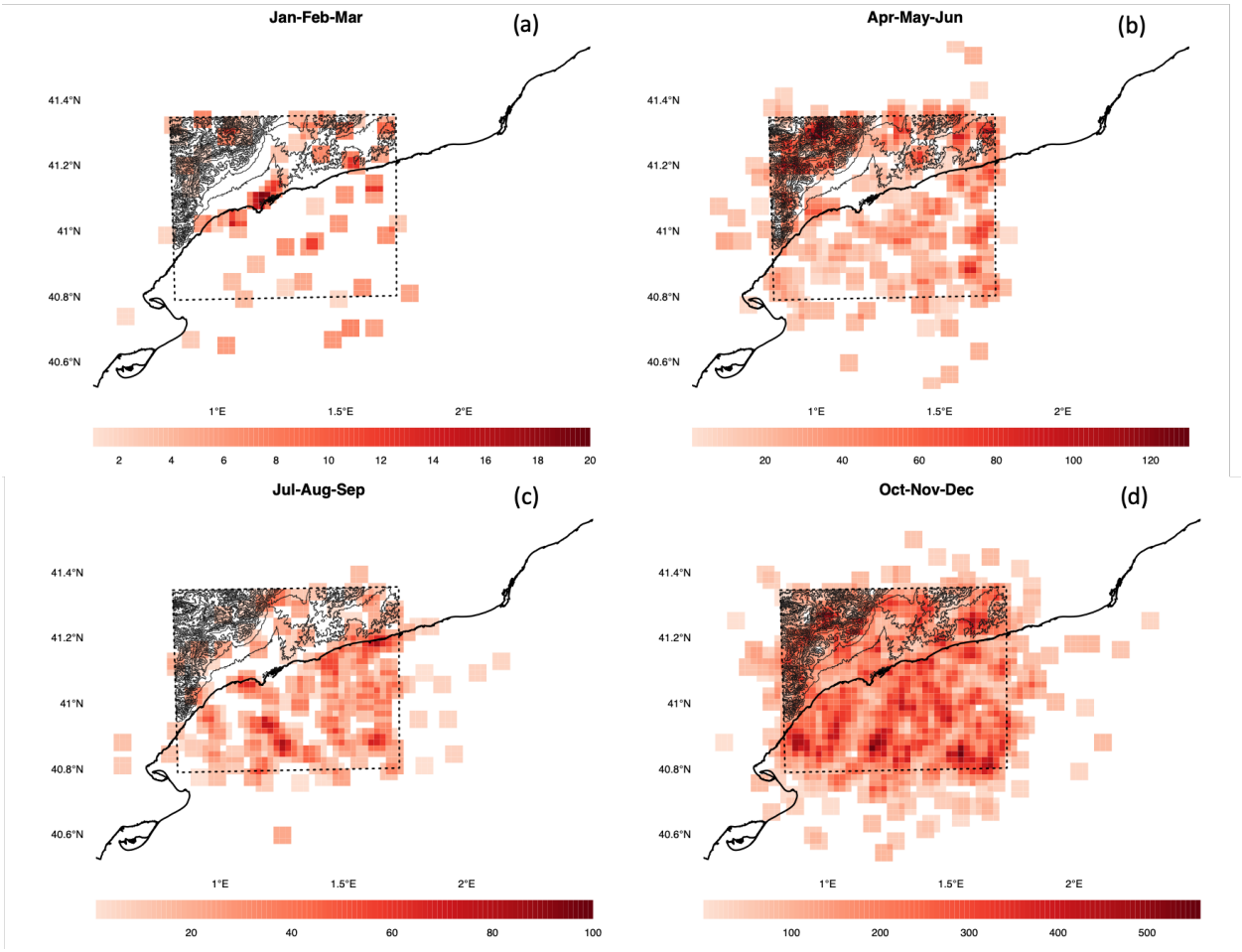

Figure 8: Spatial distribution (number of 3D cells) of storm initiation affecting ROI1, separated by season; (a) winter (January through March); (b) spring (April through June); (c) summer (July through September) and (d) Autumn (October through December). The color bar represents the number of 3D convective cells by a pixel of 2x2 km^2, and contour lines indicate the topography (every 100 m). The original pixel has been resized by applying a 3x3 Gaussian filter around it, which is why the area represented is bigger than the ROI1 area (dotted line).

4.2.2 Storm characteristics

The storm characteristics in terms of lifetime duration, direction and mean speed are shown in Fig. 9. The wind rose shows the proportion of time (in percent, %) that the wind is from a given angle and the wind speed range. In other words, it indicates where the storm comes from (e.g., a west direction in the wind rose implies that the storm is moving towards east). The median value of the entire dataset for the duration of the storms is 24 minutes, with the longest values found in the storms of 2016 in April, where the third quartile is up to 50 minutes (Fig. 9a). Then, most of the storms are singular, short-lived cells but very effective in terms of precipitation or, on the other hand, they are embedded in multicell systems. This latter case is usually associated with the convective train effect in the area (several cells are constantly growing in the rear flank and are being fed by the mature cells in the forward flank, Doswell et al., 1996). Although no satellite or broader radar image is provided in the present study, these characteristics match with other

previous studies of flash flood and mesoscale systems in the Catalan coast, where the train effect is clearly depicted (see for instance, Rigo et al., 2007; del Moral et al., 2017b or Rigo et al., 2019). It is important to remark the high monthly variability of speed and direction of the storms. Although most of the cells come from SSE or SW directions during convective season (Fig. 9b), implying that they travel from the sea to inland or parallel to the coastline, it is shown how another main direction is taken during June and August; NNE. This implies that during those months, cells could be more forced by north-eastern flow which could correspond to cold fronts crossing Catalonia.. Besides, a large proportion of the total set (more than 10%) travel from SSW towards NNE, which is exactly the coastline orientation. On respect the velocities, most of them range from 2.5 to 17 m·s-1, with the biggest segments, in all paddles, between 7.5 to 12 m·s-1, especially in October and November. This indicates that most of the storms move with the same average velocity than the flow at low levels (usually taken at 850 hPa) which would lead the storm core motion (in these cases almost surface, see for instance del Moral et al., 2018). This agrees with some previous case studies analyzed in the southern Catalan coast during autumn, that is, linearly organized mesoscale systems with convective cells that regenerate continuously, travelling mostly parallel to the coast. These systems can cross the entire Catalan region in less than 3 hours (Rigo et al., 2019), and are usually the result of Mediterranean lows. However, in other cases, they can remain stationary in located areas (Rigo and Llasat, 2005), as it is seen in other months that present low velocities (less than 2.4 $m \cdot s^{-1}$).

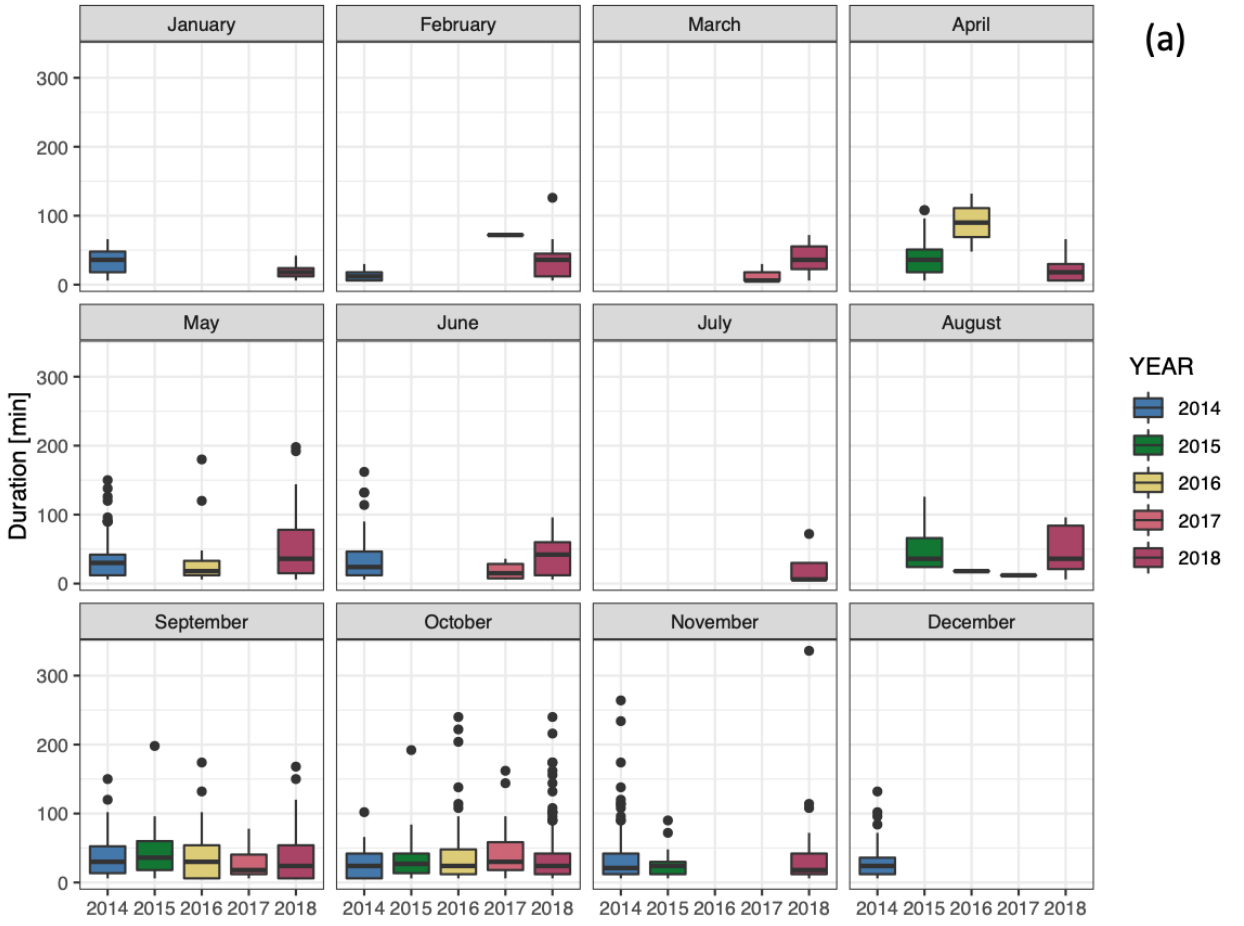

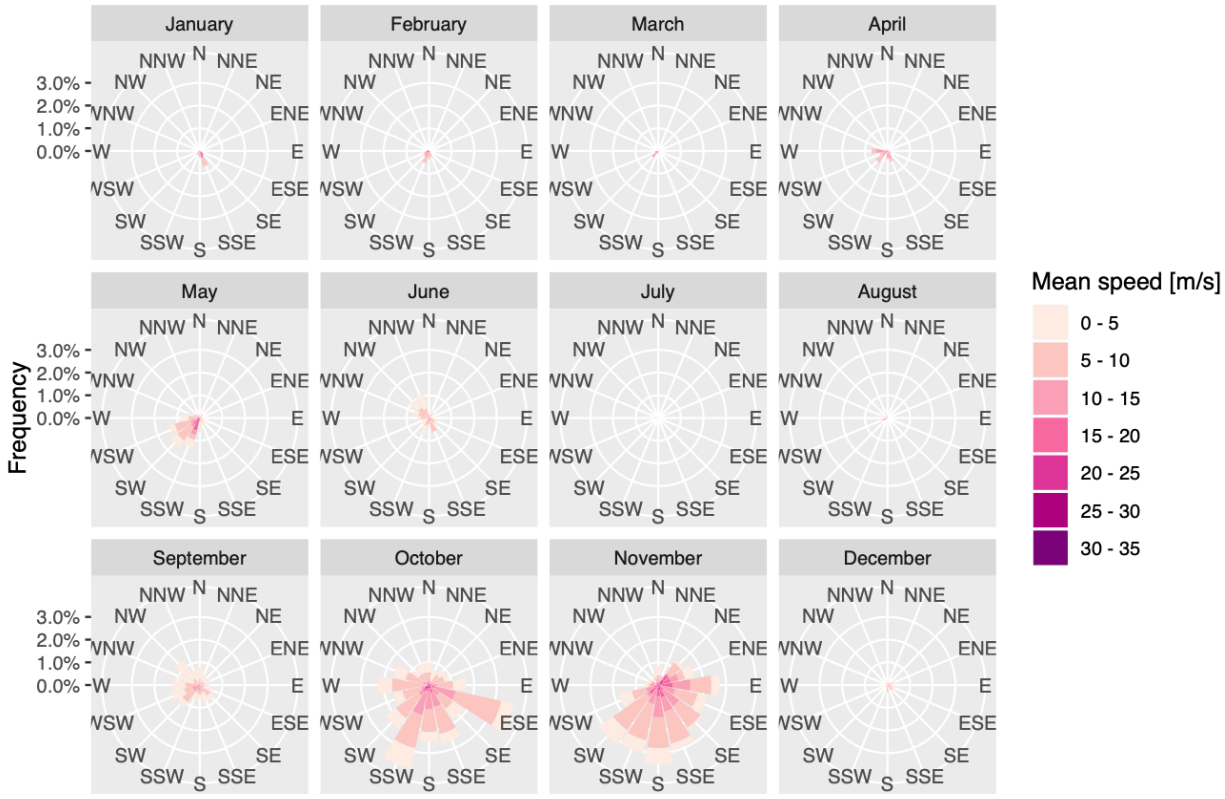

Figure 9: Storm life cycle characteristics; (a) lifetime duration [min] by months and year; (b) wind rose diagram for the total period 2014-2018, showing the frequency of storm speed [m·s^{-1}], and direction by month.

4.3 Convective characteristics in flash flood events

4.3.1 Event overview

This section focuses on the analysis of three flash flood events that affected the town of Salou and its surrounding area during the period from 2014-2018. The aim is the presentation of the main hydrologic-meteorological features, which will be compared with the thunderstorm's properties in the following section. The three cases compared and evaluated are: 29 November 2014, 29 September 2015 and 10 October 2018. The first affected the entire Catalan coast over three days, in which during the first day the system moved over the region of interest and recorded the maximum precipitation among all the cases: 336.1 mm in 24 hours in Els Ports, which is approximately 100 km south of Salou. The entire system produced several flash floods in the Catalan region, especially along the coastline. The effects of the episodes were also aggravated by the strong sea surf. In total, 179 municipalities were severely impacted, one death was recorded and the "Consorcio de Compensación de Seguros" (CCS, 2018), which is the National Insurance Company, paid more than 12.4M€ (adjusted to 2015). Although the flash flood event of 29 September 2015 only reached 145.1 mm in 24 hours in Sant Pere Pescador, North of Catalonia, it

was coincident with a strong storm surge and the CCS paid more than 12.1 M€. In this case, AWS VQ, in Constantí, approximately 20 km N of the city center of Salou, recorded a maximum precipitation of 83 mm. The Torrent de Barenys in Salou overflooded and the sea surf destroyed part of the town's seafront. Finally, during the 10 October 2018 event, additional surrounding Autonomous Communities were impacted, and the flash floods and storm surge resulted in three deaths. For this case, the maximum precipitation recorded for the region of study was 98.4 in the AWS XE, in Education Center in Tarragona, approximately 10 km N of the city center of Salou. The major affectations involved several other cities, especially Barcelona, were main roads and metro stations were flooded due to localized and intense storms. In this case, the CCS had to pay more than 2.1M€ just for the claims from the 10 October 2018 case.

The daily estimation of precipitation for ROI1, using a statistical combination of the radar field and AWS data of the SMC (del Moral et al., 2017; Rigo et al., 2019), is shown in Fig. 10. The rainfall field presents large differences between episodes, both in the distribution and in the maximum values over Salou and the surrounding area. In the case of 29 November 2014, rainfall over the city was relatively scarce, with the maximum values concentrated in the mountainous areas of the Pre-Littoral range (maximum height close to 1,200 m). In the 29 September 2015 case, the maximum values were mainly concentrated along the oriental slope of the mountain (heights lower 500 m) closer to Salou, but again the precipitation recorded over the city was low. Finally, in the 10 October 2018 case, the precipitation was situated over the town and surrounding areas. In the two first cases, flash floods started in the upper part of the streams, causing damage outside and inside the cities, while the third case was a typical example of water floods by precipitation in situ.

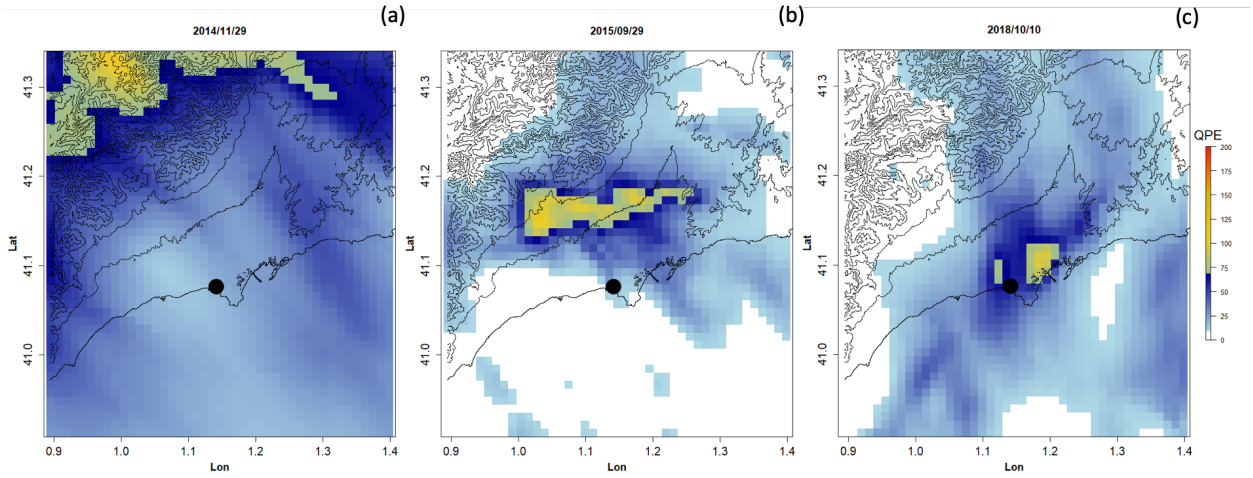

Figure 10: Estimated daily rainfall field [mm/24h], resulting from a combination of radar and rain gauges from the SMC; (a) 29 November 2014; (b) 29 September 2015; and (c) 10 October 2018. The black dot shows the location of Salou.

4.3.2 Convective characteristics

The convective cells characteristics for the three cases are shown in Fig. 11. The 2018 event shows higher values for all three characteristics (ZMAX, HTOP, and HTOP40) compared to the climatology (Fig. 5). The HTOP values span between 3 and 6 km (Fig. 11 a), with an outlier of 7 km, the HTOP40 values range from 4 to 5 km (Fig. 11 b), and the ZMAX interquartile and median

values are between 48 and 58 dBZ (Fig. 11c). These three features lie outside of the median values found for that year, (Fig. 5c) even if we consider that 2018 is an outlier among the period. This indicate that the cells affecting the area had very high rainfall intensity due to the deep vertical developments. For the two other cases (2014 and 2015), cells characteristics lie within the climatic patterns found previously from the entire year (red and orange box in Fig.5). Specifically, the vertical development (HTOP and HTOP40) range from 3-4 km (Fig. 11 a and b), and therefore suggests shallow development. However, Fig. 11c also shows that 2014 could be also considered to be slightly deviated from the median patterns in terms of cell intensity (ZMAX). In this case, the ZMAX values are higher than 45 dBZ, with a median value almost reaching 48 dBZ, indicating that the cells had shallow vertical developments but were very efficient in precipitation and with high intense rainfall (high amount of water in a short period of time).

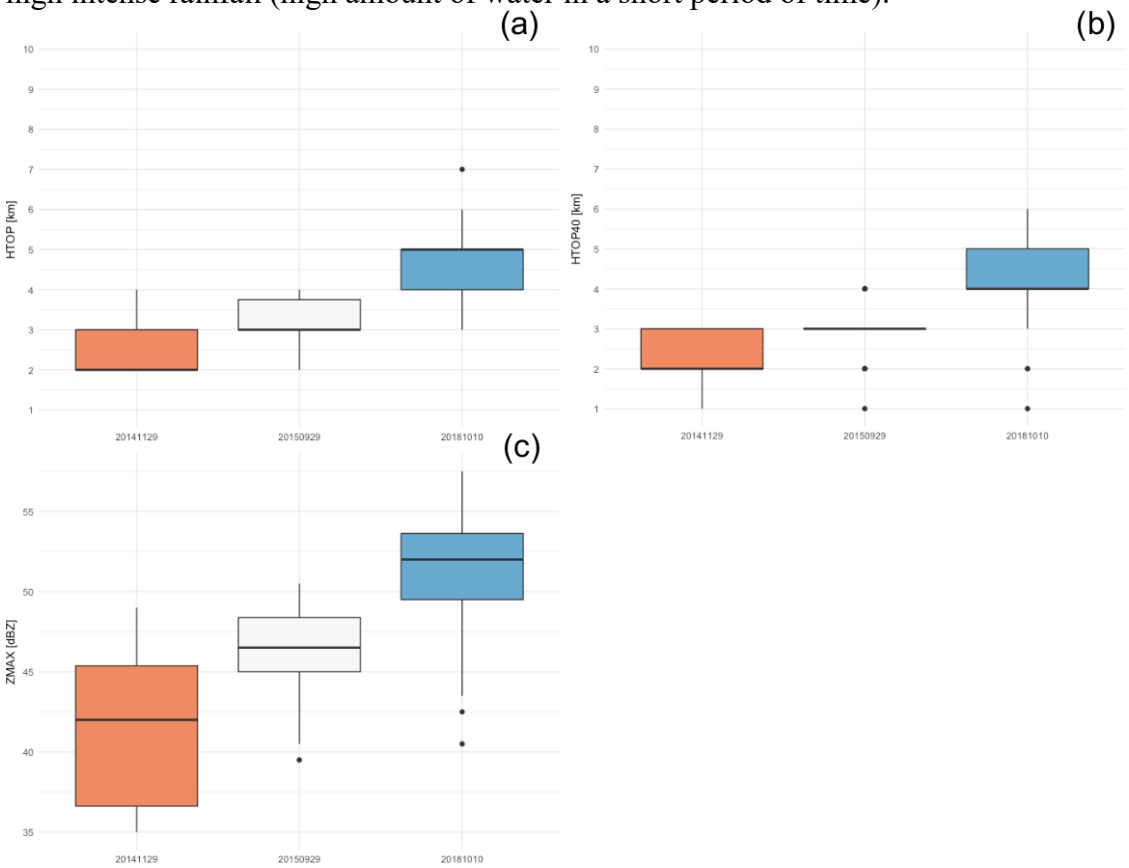

Figure 11: Characteristics of the convective cells for the three flash flood events; (a) HTOP [km], (b) HTOP40 [km] and (c) ZMAX [dBZ].

The spatial distribution of the totality of convective cells in 24 hours for the three cases, in terms of the centroid height (in blue and green pixels) and location (in red dots) is shown in Fig. 12. In this case, we show another feature resulting from the 3D identification to see if the center of mass of the entire volumetric structure coincides with the HTOP40. The centroid is computed by weighting the reflectivity values in every level by its water content (Martín et al., 2007). Convective cells of the same storm are connected with lines and arrows in Fig. 12, with the latter pointing towards the storm motion (an arrow connects cell from starting to ending point, indicating the bearing direction). The distribution is coincident with the rainfall estimation in Fig. 10 and the main vertical developments shown in Fig. 11, but also allows an understanding of some of the

behaviors in terms of motion and probable topography interaction. In 2014 and 2015, the centroid heights (big pixels in Fig. 12) were between 1 and 2.5 km (see color bar). This matches with Fig. 11 and indicate that precipitation was coming from that height. On the other hand, the cells had centroids over 3 km in 2018, with the HTOP40 and HTOP values even higher. This indicates that the maximum reflectivity occurred in a mixed-phased region with reduced liquid water content (Sui et al., 2007)

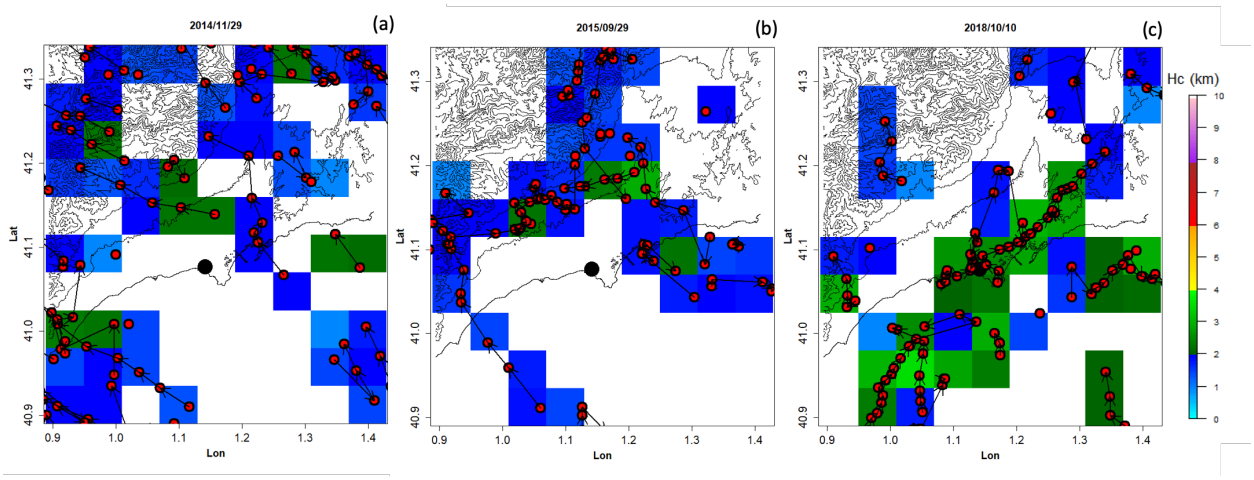

Figure 12: Spatial distribution of the totality of convective cells in 24 hours for the three events; (a) 29 November 2014; (b) 29 September 2015; and (c) 10 October 2018. Large pixels (5x5 km^2) and red dots represent the height and location of the centroid, respectively; lines and arrows represent the storm trajectory, indicating bearing direction. The black dot shows the location of Salou.

We also compare the motion and speed of the storms in these cases. In the 2014 case, it is clear from Fig. 12a that storms moved from the sea to inland (SSE to NNW), which matches with Fig. 13a. Fig. 12b then shows that the 2015 storms moved more erratically, which also can be seen in Fig. 13b. Although some of the short-lived storms over the sea show a SSE-NNW direction, it is noticeable that the storms inland, especially those interacting with the oriental slope of the mountain, present quasi-stationary motions (all dots are close in the same area and weak velocities of 0 to 2.5 m·s^{-1} from NNE to SSW in Fig. 13b. Finally, Fig. 12c and Fig. 13c show that most of the storms during the 2018 case were parallel to the coastline and had higher, although expected, speeds (5 to 10 m·s^{-1}) with SSW- NNE motion. Also, the duration of the life cycle of the storms was slightly longer compared to the climatology from Fig. 9 a (not shown), with an interquartile value ranging from 30 to 90 minutes, which is higher than the climatic value where the interquartile ranges from 10 to 50 minutes (Fig. 9a). This can be associated to a higher organization of the convection, on respect to the rest.

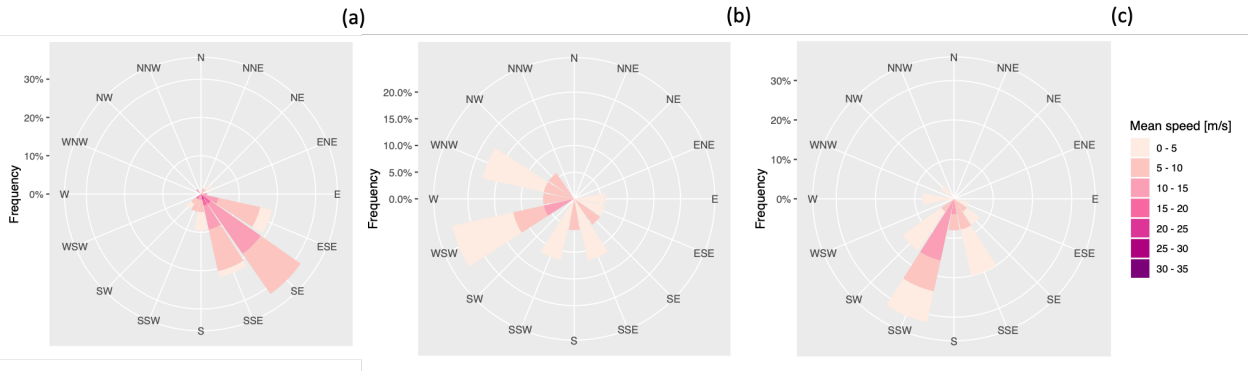

Figure 13: Wind rose diagram for the cases of study, showing the frequency of storm speed [m·s^{-1}], and direction; (a) case of 2014; (b) case of 2015; (c) case of 2018.

5. Conclusions and future work

The coastal town of Salou in the northwestern Mediterranean region has been used as a test area for analyzing different types of flash floods. It meets all the conditions of a very densely populated area, surrounded by a complex topography and a short response hydrologic basin, which is affected by different types of rainfall events. Having in mind that most of these factors can increase the vulnerability of the area in the future, it is necessary to understand the current meteorology for minimizing the impact of future climate scenarios. The analysis has been made using an algorithm for identifying, characterizing and tracking convective cells with volumetric radar data. The technique has been applied to the entire period 2014-2018, obtaining the main convective features of the area, resulting in a climatic and statistical analysis of the entire dataset. Finally, considering a database of floods in the region of study, three main events have been selected within the period studied. This has been done in order to determine the properties (intensity, duration, direction, and triggering factor) of the convection involved in those events, and to discern whether they are the result of rare storms or a common pattern in the area to be aware of. The results found in the present work can be extrapolated to other Mediterranean areas with similar characteristics.

The analysis of the convective cells and subsequent storms affecting the area shows a highest activity between September and November, with moderated reflectivity values (~40 dBZ) and low vertical developments (median of 4 km). Also, these are mainly initiated over the sea or the coastline, travelling or either to inland or parallel to the coastline, and with relatively high velocities. This likely corresponds to a convective train effect in multicell or mesoscale systems; new developing cells are being fed by the stationary cold pool of the mature and dissipating ones (preceding). This, along with the configuration of the mean wind and cells' motion inside the system, makes the region to be constantly affected by rain in large periods of time. This is a completely different regime, for instance, as the one affecting the plains or mountain areas in Catalonia, where isolated deep convection produces mostly severe weather (hail or strong wind). Furthermore, the sea is demonstrated to play a major role in the efficiency of the precipitation. The configuration demonstrates the particularity of this coastal area, with shallower convection and a different general flow compared to other areas of Catalonia (Rigo et al., 2010; del Moral et al., 2018; Rigo and Llasat, 2018).

In general, and for the analyzed flood events, cells show the main pattern studied in the ROI; shallow and efficient convection due to the proximity to the sea, playing an important role in the total accumulated values. However, the topography also favors three main key aspects that can be seen from the analysis of the 2018 case, the one that differs from the general pattern. First, it allows the triggering of the convection in those cases where the instability is not high; second, it helps in the formation of an instability line over which the thunderstorms grow, and third, it becomes a capping feature for the cells that get to pass the coastline. This last factor points out that not just a better weather warning system is needed for the area, but also a good adaptation infrastructure plan. Even if the area is not affected by continuous efficient rainfall, flash floods may happen if storms are blocked upstream, producing a rapid increase in the flow in the small streams flooding the settlements (catchments results saturated by a large amount of water).

The results match with other studies done previously in other parts of the world. Shallow and efficient convection has been broadly analyzed in many regions, prevailing in the Tropic and Sub-Tropic areas (see, for instance, Short and Nakamura, 2000; Pereira and Rutledge, 2006; or Schumacher and Houze Jr., 2003). The shallow convective cells in these regions are characterized by echo tops usually near 2 km, notably lower than the observed in our region, which could be explained by the presence of a freezing level higher than 3 km (clearly over the one found in the Catalan area). Besides, another important point is the notable contribution of this type of precipitation in the total amount of rainfall; between 10% and 30%, depending on the region. Having in mind that some of the cases that produce the maximum accumulation values in our area of study are produced by this type of precipitation, it could be possible that, in some coastal areas of the Mediterranean, these percentages are even larger. It is also important to highlight that the results here presented are similar to those observed in the analysis of the rainfall regimes in Australia (May and Ballinger, 2007), where a high number of short-lifetime shallow cells are found. They also match with the cells observed in Israel (Eastern Mediterranean) by Peleg and Morin (2012), where it is found a large contribution of the sea in the development of shallow convection. Godart et al. (2011) observed the importance of the topography in the south of France in the evolution of shallow convection, which also represents the highest contribution in the total rainfall amount for that area.

The work here presented demonstrates the need of a weather early warning system in conjunction with adaptation plans. The results so far show that from the meteorological aspects, the system should consider fast recognition of convective cells, accounting for the intensity, that can be translated to precipitable water, but also the motion coupled with the topography. It should be able to set different risk levels depending on two main areas; upstream and downstream of the catchment, since they need differenced precipitation threshold. Furthermore, the system should be able to release weather warnings if the cells are stationary in the same area for a long time. In this sense, the authors consider that the new 3D identification and tracking tool used in this research (del Moral et al., 2018), and that is now being put into the operative system in the Meteorological Service of Catalonia, would be a base tool for the warning system. Although there's still a need to address the issue found with the non-weather clutter echoes, which may give false alarms if the threshold is set to values too high, the authors consider that radar-based nowcasting is the good approach to this type of convection and the related phenomena. This also matches with similar analysis that have been made in Central Europe by Trentmann et al. (2009), which showed that numerical models are only able to reproduce the nature of the environment, but not to identify the

position and time of occurrence of the shallow and efficient convective cells nor either the total accumulation that these produce.

The present research also opens the door to more future work that needs to be done. It is necessary to extend the current work to other risk areas to know if the convective patterns found in the coast of Salou (south of Catalonia) are also found in regions with similar orographic and social configuration, such the Maresme coast (north of Catalonia). In this sense, the warning system could be extended to the entire coastal region (sensible to future scenarios). Also, the authors consider that future studies should include research on some of the key features that have appeared in this preliminary one: the efficiency of the precipitation, the role of the sea and topography and the motion of the systems. This suggests doing a broad study of the thermodynamic and synoptic and mesoscale conditions of storms affecting the area, which could be done by means of the new ERA5 reanalysis dataset (from 1979 to within 3 months of real time) and for public use, recently released (C3S, 2017). First, we consider that some of the convective patterns found could be related to warm precipitation (Lin et al., 2001; Liu et al., 2009) and therefore a knowledge of features such as associated lightning and the height of the 0º isotherm would polish the actual convective definition in the area. The latter would help to understand where the melting level is located and therefore the contribution of liquid and/or ice particles in the rain, as well as efficiency. Finally, it would be important to know which has been the main weather type associated to these convective events in the past years, following the work done by Llasat et al. (2005) and Gilabert and Llasat (2017), and how this could change in future scenarios. This would allow computing the impact in low level winds configuration and sea surface temperature changes and sharpen the future warning systems and adaptation measures. Also, this could confirm the results found previously by Atkinson and Zhang (1996) about shallow convection (cells from 1 to 2 km, with an extend of less than few tens of kilometers), or Kirshbaum and Durran (2004) which investigated how the potential instability, the height of the mountain barrier, the altitude of the unstable layer or the wind shear may affect the development of this type of convection.

Acknowledgements

The study has been developed in the framework of the Spanish National Project M-CostAdapt (CTM2017-83655-C2-2-R). The authors want to thank Montse Llasat-Botija and Maria Cortés Simó for their contribution and information about the flash flood events that affected the region of study, to XXX for providing the AWS and historical data of the Meteorological Service of Catalonia, and to McKenna W. Stanford for the thorough English review and helpful scientific suggestions.

References

Altube, P., Bech, J., Argemí, O., Rigo, T., 2015. Quality control of antenna alignment and receiver calibration using the sun: Adaptation to midrange weather radar observations at low elevation angles. J. Atmos. Ocean. Technol. 32, 927–942.

Aran, M., Peña, J.C., Pineda, N., Soler, X., Pérez-Zanón, N., 2015. Ten-year lightning patterns in Catalonia using Principal Component Analysis.

Atkinson, B. W., & Wu Zhang, J. (1996). Mesoscale shallow convection in the atmosphere. Reviews of Geophysics, 34(4), 403-431.

Ballart, D., Figuerola, F., Aran, M., & Rigo, T. (2009, September). Analysis of warm convective rain events in Catalonia. In 11th Plinius Conference on Mediterranean Storms, held September 7-10, 2009 in Barcelona, Spain. http://meetings. copernicus. org/plinius11, id. Plinius11-115.

Barnolas, M., Llasat, M.C., 2007. A flood geodatabase and its climatological applications: the case of Catalonia for the last century. Nat. Hazards Earth Syst. Sci. 7, 271–281.

Braud, I., Bouvier, C., Branger, F., Delrieu, G., Le Coz, J., Nord, G., Vandervaere, J.-P., Anquetin, S., Adamovic, M., Andrieu, J., Batiot, C., Boudevillain, B., Brunet, P., Carreau, J., Confoland, A., Didon-Lescot, J.-F., Domergue, J.-M., Douvinet, J., Dramais, G., Freydier, R., Gérard, S., Huza, J., Leblois, E., Le Bourgeois, O., Le Boursicaud, R., Marchand, P., Martin, P., Nottale, L., Patris, N., Renard, B., Seidel, J.-L., Taupin, J.-D., Vannier, O., Vincendon, B., Wijbrans, A., 2014. Multi-scale hydrometeorological observation and modelling for flash flood understanding. Hydrol. Earth Syst. Sci. 18, 3733–3761.

Corral, C., Velasco, D., Forcadell, D., Sempere-Torres, D., Velasco, E., 2009. Advances in radar-based flood warning systems. The EHIMI system and the experience in the Besòs flash-flood pilot basin.

Cortés Simó, M., Turco, M., Llasat-Botija, M., Llasat Botija, M. del C., 2018. The relationship between precipitation and insurance data for floods in a Mediterranean region (northeast Spain). Nat. Hazards Earth Syst. Sci. 2018, vol. 18, p. 857-868.

Cortès, M., Gilabert, J., Llasat-Botija, M., Marcos, R., Llasat, M. del C., 2017. Urban and peri-urban flood impact change: the case of the Metropolitan Area of Barcelona, in: EGU General Assembly Conference Abstracts. p. 762.

Cramer, W., Guiot, J., Fader, M., Garrabou, J., Gattuso, J.-P., Iglesias, A., Lange, M.A., Lionello, P., Llasat, M.C., Paz, S., 2018. Climate change and interconnected risks to sustainable development in the Mediterranean. Nat. Clim. Chang. 8, 972–980.

(C3S), C.C.C.S., 2017. ERA5: Fifth generation of ECMWF atmospheric reanalyses of the global climate.

Consorcio de Compensación de Seguros,1971. Estadística de riesgos extraordinarios. Serie 2010, 80–81.

del Moral, A., del Carmen Llasat, M., Rigo, T., 2017a. Identification of anomalous motion of thunderstorms using daily rainfall fields. Atmos. Res. 185, 92–100.

del Moral, A., Cortès M., del Carmen Llasat, M., Rigo, T., 2017b. The 12th October 2016 Maresme flash-floods: a radar-based analysis. Poster in: 10th HyMeX Workshop, 4-7 July 2017, Barcelona, Spain. DOI:10.13140/RG.2.2.14826.82889del Moral, A., Rigo, T., Llasat, M.C., 2018a. A radar-based centroid tracking algorithm for severe weather surveillance: identifying split/merge processes in convective systems. Atmos. Res. 213, 110–120.

del Moral, A., Rigo, T., Llasat, M. C., 2018b. Performance of a new algorithm for nowcasting anomalous trajectories. Proceeding in: 10th European Conference on Radar in Meteorology and Hydrology (ERAD 2018), 1- 6 July, Ede-Wageningen, The Netherlands. DOI: 10.18174/454537

Dixon, M., Wiener, G., 1993. TITAN: Thunderstorm identification, tracking, analysis, and nowcasting—A radar-based methodology. J. Atmos. Ocean. Technol. 10, 785–797.

Doswell III, C.A., Brooks, H.E., Maddox, R.A., 1996. Flash flood forecasting: An ingredients-based methodology. Weather Forecast. 11, 560–581.

Doswell, C.A., 2001. Severe convective storms—An overview, in: Severe Convective Storms. Springer, pp. 1–26.

Ducrocq, V., Braud, I., Davolio, S., Ferretti, R., Flamant, C., Jansa, A., Kalthoff, N., Richard, E., Taupier-Letage, I., Ayral, P.-A., 2014. HyMeX-SOP1: The field campaign dedicated to heavy precipitation and flash flooding in the northwestern Mediterranean. Bull. Am. Meteorol. Soc. 95, 1083–1100.

Farnell, C., Rigo, T., Pineda, N., 2017. Lightning jump as a nowcast predictor: application to severe weather events in Catalonia. Atmos. Res. 183, 130–141.

Fiori, E., Comellas, A., Molini, L., Rebora, N., Siccardi, F., Gochis, D.J., Tanelli, S., Parodi, A., 2014. Analysis and hindcast simulations of an extreme rainfall event in the Mediterranean area: The Genoa 2011 case. Atmos. Res. 138, 13–29.

Gaume, E., M. Borga, M.C. Llasat, S. Maouche, M. Lang, M. Diakakis, 2016. Mediterranean extreme floods and flash floods. Into Hydro-meteorological extremes, chapter 3, The Mediterranean Region under Climate Change. A Scientific Update (coordinated byAllEnvi).133-144. IRD Éditions Institut de Recherche pour le Développement, Marseille, 2016, ISBN : 978-2-7099-2219-7.

Gilabert, J. and M.C. Llasat, 2017. Circulation weather types associated with extreme flood events in Northwestern Mediterranean. Int. J. Climatol. (2017) Published online in Wiley Online Library (wileyonlinelibrary.com) DOI: 10.1002/joc.5301

Godart, A., Anquetin, S., Leblois, E., & Creutin, J. D. (2011). The contribution of orographically driven banded precipitation to the rainfall climatology of a Mediterranean region. Journal of Applied Meteorology and Climatology, 50(11), 2235-2246.

Han, L., Fu, S., Zhao, L., Zheng, Y., Wang, H., Lin, Y., 2009. 3D convective storm identification, tracking, and forecasting—An enhanced TITAN algorithm. J. Atmos. Ocean. Technol. 26, 719–732.

Hu, J., Rosenfeld, D., Zrnic, D., Williams, E., Zhang, P., Snyder, J.C., Ryzhkov, A., Hashimshoni, E., Zhang, R., Weitz, R., 2019. Tracking and characterization of convective

cells through their maturation into stratiform storm elements using polarimetric radar and lightning detection. Atmos. Res. 226, 192–207.

Johnson, J.T., MacKeen, P.L., Witt, A., Mitchell, E.D.W., Stumpf, G.J., Eilts, M.D., Thomas, K.W., 1998. The storm cell identification and tracking algorithm: An enhanced WSR-88D algorithm. Weather Forecast. 13, 263–276.

Kirshbaum, D. J., & Durran, D. R. (2004). Factors governing cellular convection in orographic precipitation. Journal of the atmospheric Sciences, 61(6), 682-698.Kumjian, M.R., Ryzhkov, A. V, 2008. Polarimetric signatures in supercell thunderstorms. J. Appl. Meteorol. Climatol. 47, 1940–1961.

Lin, Y.-L., Chiao, S., Wang, T.-A., Kaplan, M.L., Weglarz, R.P., 2001. Some common ingredients for heavy orographic rainfall. Weather Forecast. 16, 633–660.

Liu, C., Zipser, E.J., 2009. "Warm rain" in the tropics: Seasonal and regional distributions based on 9 yr of TRMM data. J. Clim. 22, 767–779.

Llasat, M.C., Llasat-Botija, M., Rodriguez, A., Lindbergh, S., 2010a. Flash floods in Catalonia: a recurrent situation. Adv. Geosci. 26, 105–111.

Llasat, M.C., Llasat-Botija, M., Prat, M.A., Porcu, F., Price, C., Mugnai, A., Lagouvardos, K., Kotroni, V., Katsanos, D., Michaelides, S., 2010b. High-impact floods and flash floods in Mediterranean countries: the FLASH preliminary database. Adv. Geosci. 23, 47–55.

Llasat, M.C., Marcos, R., Llasat-Botija, M., Gilabert, J., Turco, M., Quintana-Seguí, P., 2014. Flash flood evolution in north-western Mediterranean. Atmos. Res. 149, 230–243.

Llasat, M.-C., Barriendos, M., Barrera, A., Rigo, T., 2005. Floods in Catalonia (NE Spain) since the 14th century. Climatological and meteorological aspects from historical documentary sources and old instrumental records. J. Hydrol. 313, 32–47.

Llasat, M.-C., Ceperuelo, M., Rigo, T., 2007. Rainfall regionalization on the basis of the precipitation convective features using a raingauge network and weather radar observations. Atmos. Res. 83, 415–426.

Martín, F., Elizaga, F., Carretero, O., San, Ambrosio I., 2007. Diagnóstico y predicción de la convección profunda (in Spanish). In: Technical Note n. 35 of the Analysis and Forecasting Technical Service of the Spanish Weather Service, pp. 174.

May, P. T., & Ballinger, A. (2007). The statistical characteristics of convective cells in a monsoon regime (Darwin, Northern Australia). Monthly weather review, 135(1), 82-92.

Pastor, F., Valiente, J.A., Estrela, M.J., 2015. Sea surface temperature and torrential rains in the Valencia region: modelling the role of recharge areas. Nat. Hazards Earth Syst. Sci. 15, 1677–1693.

Peleg, N., & Morin, E. (2012). Convective rain cells: Radar-derived spatiotemporal characteristics and synoptic patterns over the eastern Mediterranean. Journal of Geophysical Research: Atmospheres,117(D15).

Pereira, L. G., & Rutledge, S. A. (2006). Diurnal cycle of shallow and deep convection for a tropical land and an ocean environment and its relationship to synoptic wind regimes. Monthly Weather Review,134(10), 2688-2701.

Petrucci, O., L.Aceto, C.Bianchi, V.Bigot, R. Brázdil, S.Pereira, A.Kahraman, Ö.Kılıç, V.Kotroni, M.C. Llasat, M. Llasat-Botija, K. Papagiannaki, A. A. Pasqua, J. Řehoř, J. Rossello Geli, P. Salvati, F. Vinet, J.L. Zêzere. (2019). Flood Fatalities in Europe, 1980–2018: Variability, Features, and Lessons to Learn, Water 2019, 11, 1682; doi:10.3390/w11081682

Pineda, N., Rigo, T., Bech, J., Soler, X., 2007. Lightning and precipitation relationship in summer thunderstorms: Case studies in the North Western Mediterranean region. Atmos. Res. 85, 159–170.

Pulkkinen, S., Chandrasekar, V., Harri, A.-M., 2019. Stochastic Spectral Method for Radar-Based Probabilistic Precipitation Nowcasting. J. Atmos. Ocean. Technol. 36, 971–985.

Rigo, T., Berenguer, M., del Carmen Llasat, M., 2019. An improved analysis of mesoscale convective systems in the western Mediterranean using weather radar. Atmos. Res. 227, 147–156.

Rigo, T. and Llasat, M. C. 2004: A methodology for the classification of convective structures using meteorological radar: Application to heavy rainfall events on the Mediterranean coast of the Iberian Peninsula, Nat. Hazards Earth Syst. Sci., 4, 59–68, https://doi.org/10.5194/nhess-4-59-2004, 2004.

Rigo, T., and Llasat, M.C., 2005. Radar analysis of the life cycle of Mesoscale Convective Systems during the 10 June 2000 event. Nat. Hazards Earth Syst. Sci. 5, 959–970.

Rigo, T., and Llasat, M. C. 2007. Analysis of mesoscale convective systems in Catalonia using meteorological radar for the period 1996–2000. Atmospheric Research, 83(2-4), 458-472

Rigo, T., Llasat, M.C., 2016. Forecasting hailfall using parameters for convective cells identified by radar. Atmos. Res. 169, 366–376.

Rigo, T., Pineda, N., Bech, J., 2010. Analysis of warm season thunderstorms using an object-oriented tracking method based on radar and total lightning data. Nat. Hazards Earth Syst. Sci. 2010, Vol. 10, p. 1881-1893.

Rodríguez, O., Bech, J., 2018. Sounding-derived parameters associated with tornadic storms in Catalonia. Int. J. Climatol. 38, 2400–2414.

Rozalis, S., Morin, E., Yair, Y., Price, C., 2010. Flash flood prediction using an uncalibrated hydrological model and radar rainfall data in a Mediterranean watershed under changing hydrological conditions. J. Hydrol. 394, 245–255.

Schumacher, C., & Houze Jr, R. A. (2003). The TRMM precipitation radar's view of shallow, isolated rain. Journal of Applied Meteorology, 42(10), 1519-1524.Seneviratne, S.I., N. Nicholls, D. Easterling, C.M. Goodess, S. Kanae, J. Kossin, Y. Luo, J. Marengo, K. McInnes, M. Rahimi,M. Reichstein, A. Sorteberg, C. Vera, and X. Zhang, 2012: Changes in climate extremes and their impacts on the natural physical environment. In: Managing the Risks of Extreme Events and Disasters to Advance Climate Change Adaptation [Field, C.B., V. Barros, T.F. Stocker, D. Qin, D.J. Dokken, K.L. Ebi, M.D. Mastrandrea, K.J. Mach, G.-K. Plattner, S.K. Allen, M. Tignor, and P.M. Midgley (eds.)]. A Special Report of Working Groups I and II of the Intergovernmental Panel on Climate Change (IPCC). Cambridge University Press, Cambridge, UK, and New York, NY, USA, pp. 109-230.

Shi, J., Wang, P., Wang, D., Jia, H., 2019. Radar-Based Automatic Identification and Quantification of Weak Echo Regions for Hail Nowcasting. Atmosphere (Basel). 10, 325.

Short, D. A., & Nakamura, K. (2000). TRMM radar observations of shallow precipitation over the tropical oceans. Journal of Climate, 13(23), 4107-4124.

Spekkers, M.H., Kok, M., Clemens, F., Ten Veldhuis, J.A.E., 2013. A statistical analysis of insurance damage claims related to rainfall extremes. Hydrol. Earth Syst. Sci. 17, 913–922.

Steinacker, R., Dorninger, M., Wölfelmaier, F., Krennert, T., 2000. Automatic tracking of convective cells and cell complexes from lightning and radar data. Meteorol. Atmos. Phys. 72, 101–110.

Sui, C.-H., Li, X., Yang, M.-J., 2007. On the definition of precipitation efficiency. J. Atmos. Sci. 64, 4506–4513.

Toreti, A., Naveau, P., 2015. On the evaluation of climate model simulated precipitation extremes. Environ. Res. Lett. 10, 14012.

Toreti, A., Naveau, P., Zampieri, M., Schindler, A., Scoccimarro, E., Xoplaki, E., Dijkstra, H.A., Gualdi, S., Luterbacher, J., 2013. Projections of global changes in precipitation extremes from Coupled Model Intercomparison Project Phase 5 models. Geophys. Res. Lett. 40, 4887–4892.

Torgersen, G., Bjerkholt, J. ., Kvaal, K., Lindholm, O. G., 2015. Correlation between extreme rainfall and insurance claims due to urban flooding–case study fredrikstad, norway. Journal of Urban and Environmental Engineering 9 (2), 127–138.

Tramblay, Y., Somot, S. Future evolution of extreme precipitation in the Mediterranean. Climatic Change, 151:289–302 https://doi.org/10.1007/s10584-018-2300-5 (2018)

Trapero, L., Bech, J., Rigo, T., Pineda, N., Forcadell, D., July 2009. Uncertainty of precipitation estimates in convective events by the meteorological service of Catalonia radar network. Atmos. Res. 93, 408–418.

Trentmann, J., Keil, C., Salzmann, M., Barthlott, C., Bauer, H. S., Schwitalla, T., ... & Kottmeier, C. (2009). Multi-model simulations of a convective situation in low-mountain terrain in central Europe. Meteorology and atmospheric physics, 103(1-4), 95-103.

Velasco-Forero, C. A., Sempere-Torres, D., Cassiraga, E. F., G´omez-Hern andez, J. J., 2009. A non-parametric automatic blending methodology to estimate rainfall fields from rain gauge and radar data. Advances in Water Resources 32 (7), 986–1002.